Electronic Supplementary Material (ESI) for Physical Chemistry Chemical Physics.

Combined NMR and DFT study of conformational dynamics in lanthanide DOTA-like complexes

Jan Blahut, Petr Hermann, Zdeněk Tošner, and Carlos Platas-Iglesias,

Electronic supplementary information

Content:

For all calculated Cartesian coordinates and related energies of intermediates see folder in coordinatesArchive.rar archive.

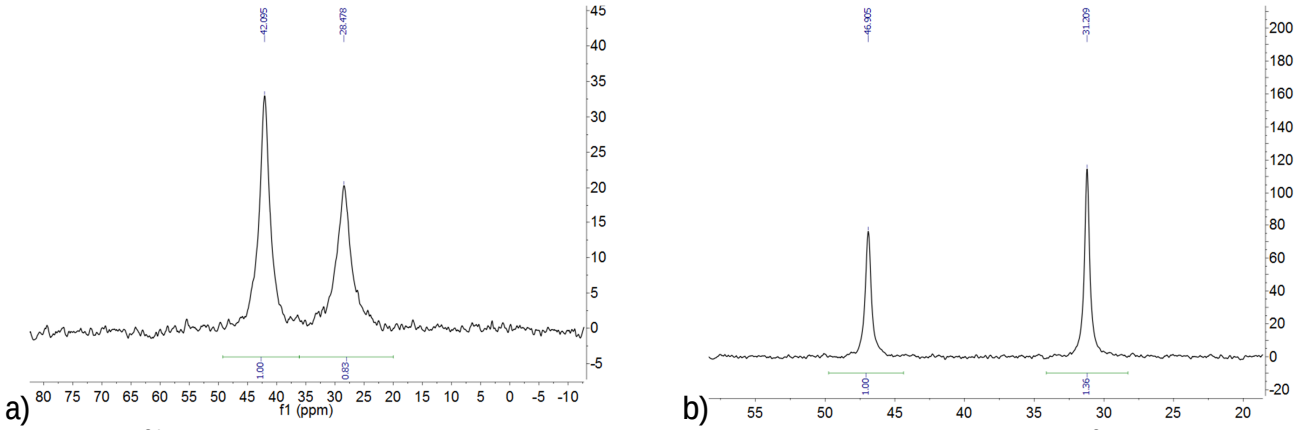

Figure S1: ^{31}P spectra of a) $[Eu(Hdo3ap)(D_2O)]^{-}$ (pD = 3.6) and b) $[Eu(Hdo3ap)(D_2O)]^{2-}$ (pD = 8.5) at 5 °C and 162 MHz.

Table S1: ^{1}H chemical shifts at 5 °C of axial and equatorial hydrogen nuclei used in 1D-EXSY studies. Supplement to Figure 2 in the main text.

δ/ppm	dota	Hdo3ap	do3ap
SAP axial 1	36.32	38.02	40.68
SAP axial 2	–	37.00	39.68
SAP axial 3	–	34.98	37.20
SAP axial 4	–	29.50	28.30
TSAP axial 1	13.78	20.74	25.16
TSAP axial 2	–	17.17	20.34
TSAP axial 3	–	11.76	12.93
TSAP axial 4	–	9.34	9.70
SAP equatorial 1	–7.04	–2.78	–1.04
SAP equatorial 2	–	–4.02	–3.15
SAP equatorial 3	–	–10.07	–10.01
SAP equatorial 4	–	–9.26	–8.43
TSAP equatorial 1	–10.06	–3.84	–4.48
TSAP equatorial 2	–	–7.83	–4.03
TSAP equatorial 3	–	–11.98	–11.32
TSAP equatorial 4	–	–14.3	–16.81

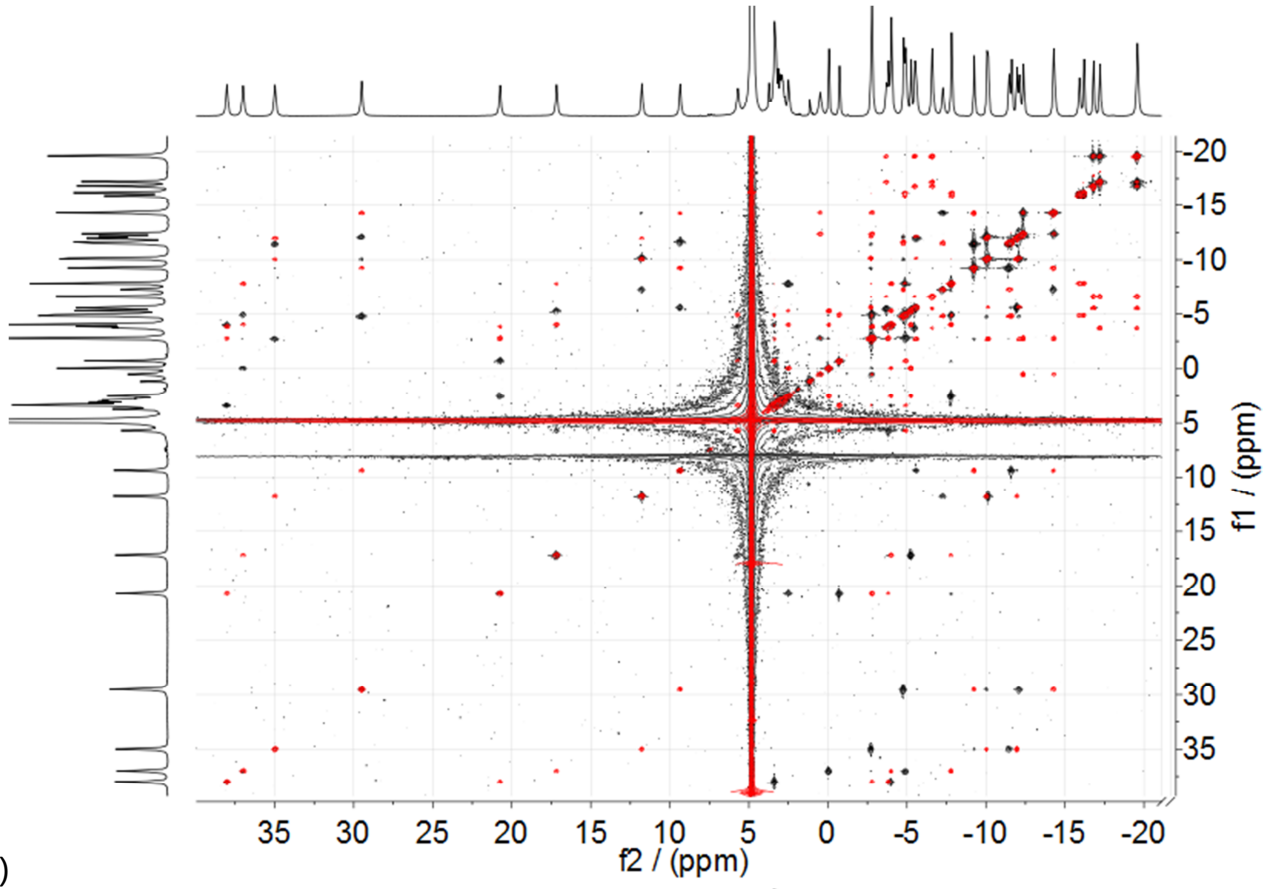

a)

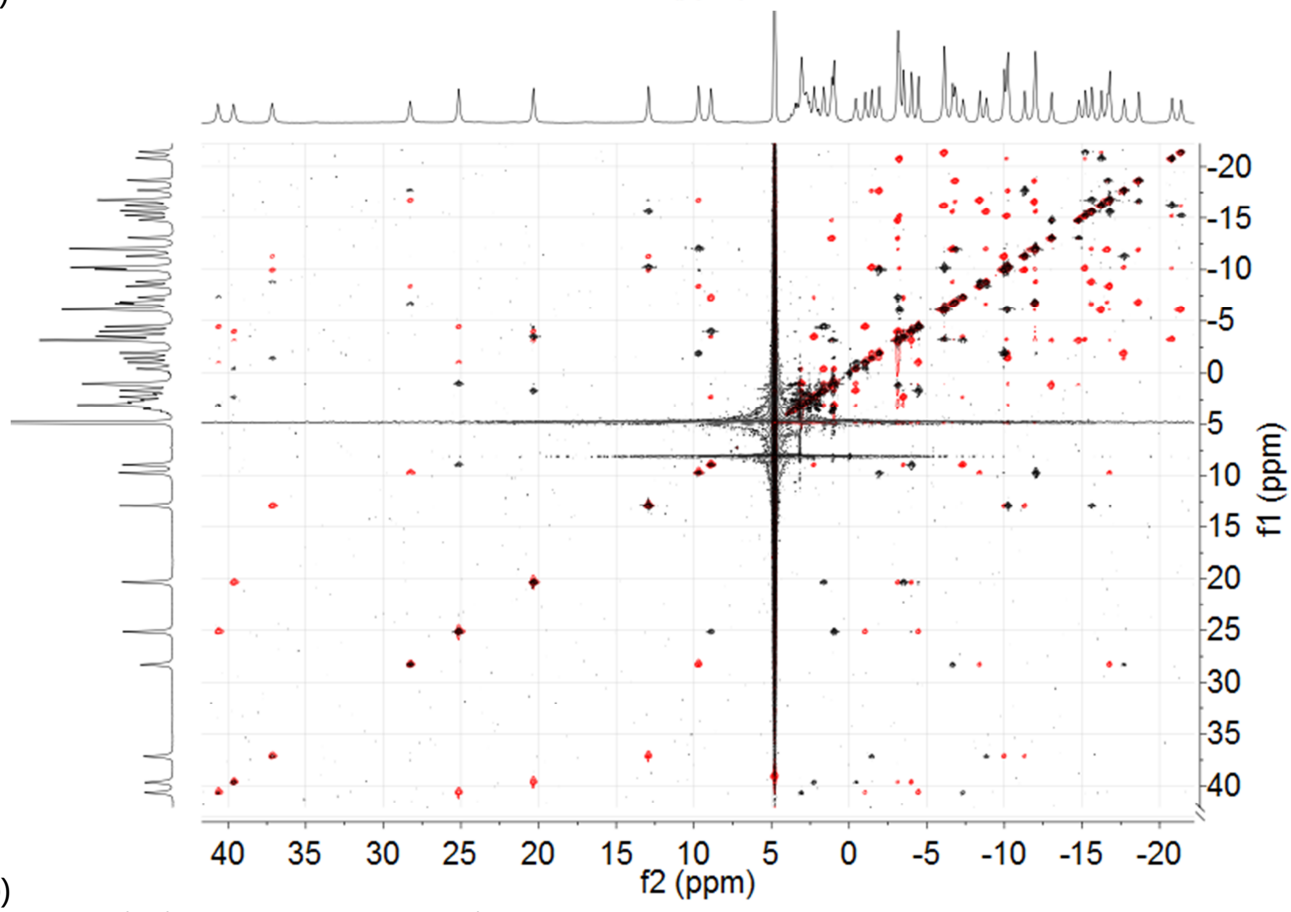

b)

Figure S2: ^{1}H-^{1}H 2D-COSY (black) and ^{1}H 2D-EXSY spectra (red) of a) $[Eu(Hdo3ap)(D_2O)]^{-}$ (pD = 3.6) and b) $[Eu(do3ap)(D_2O)]^{2-}$ (pD = 8.5); 5 °C, 600 MHz, mixing time 5 ms for (a) and 10 ms for (b).

a)

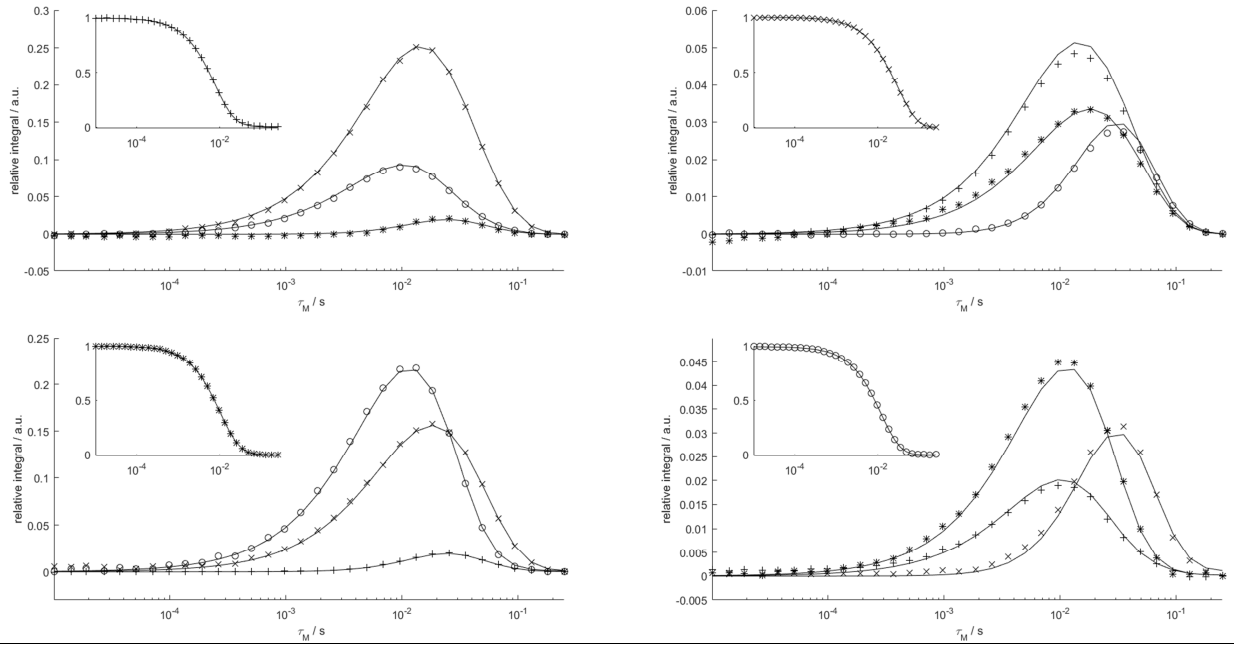

b)

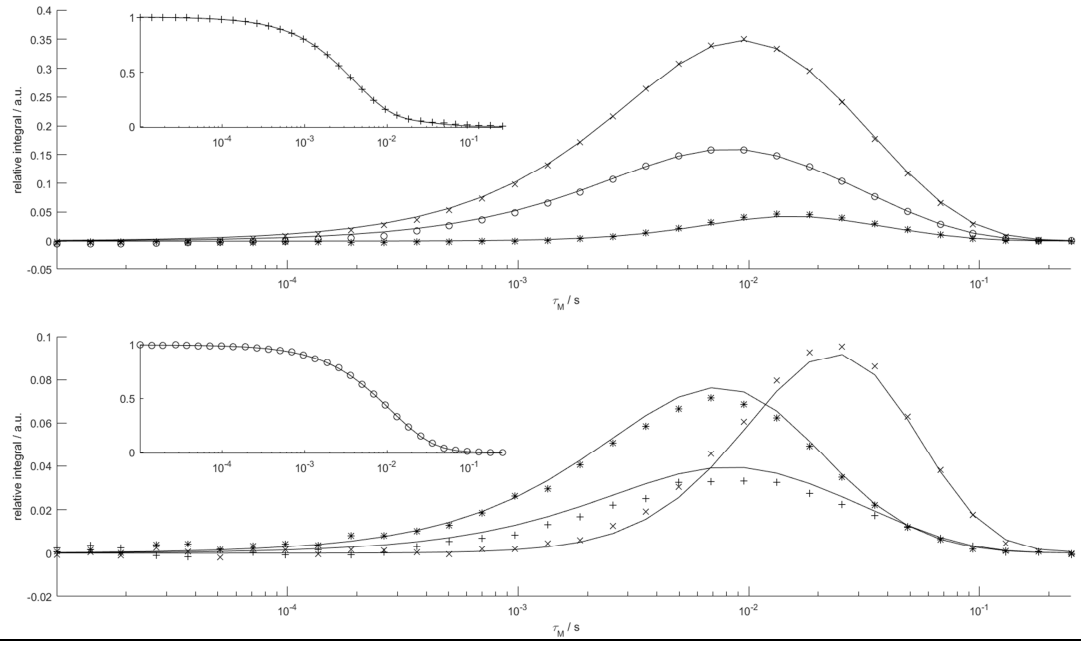

c)

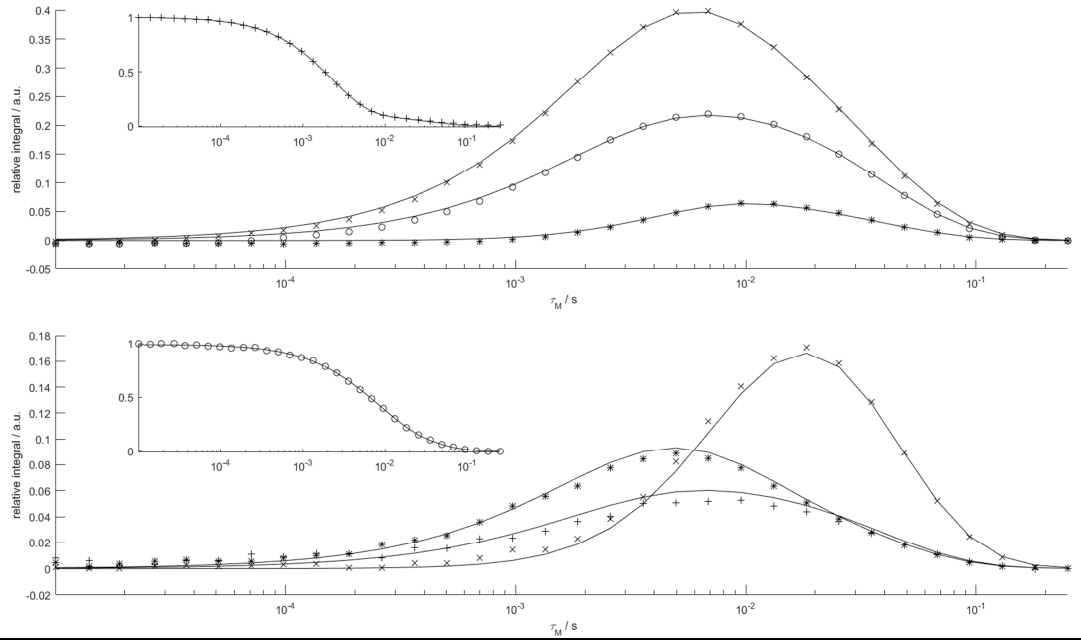

d)

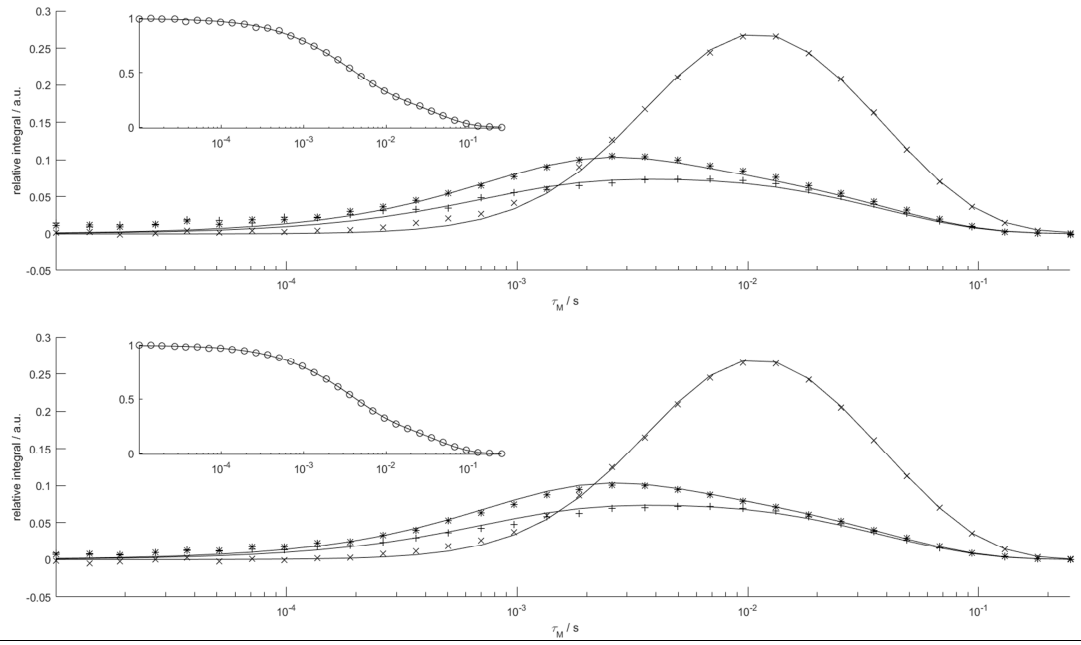

Figure S3. Relative areas of proton NMR signals of $[Eu(dota)(D_2O)]^-$ as a function of the mixing time obtained from 1D-EXSY experiments at a) 5 °C b) 15 °C c) 25 °C and d) 35 °C at pD = 7.0. The insets show the evolution of the magnetisation of the signal to which the refocusing selective 180° pulse was applied. Symbols: $TSAP_{ax}$ (+), SAP_{eq} (×), $TSAP_{eq}$ (*), SAP_{ax} (○). The solid lines represent the simultaneous fit of all four data sets using Equation [2].

a)

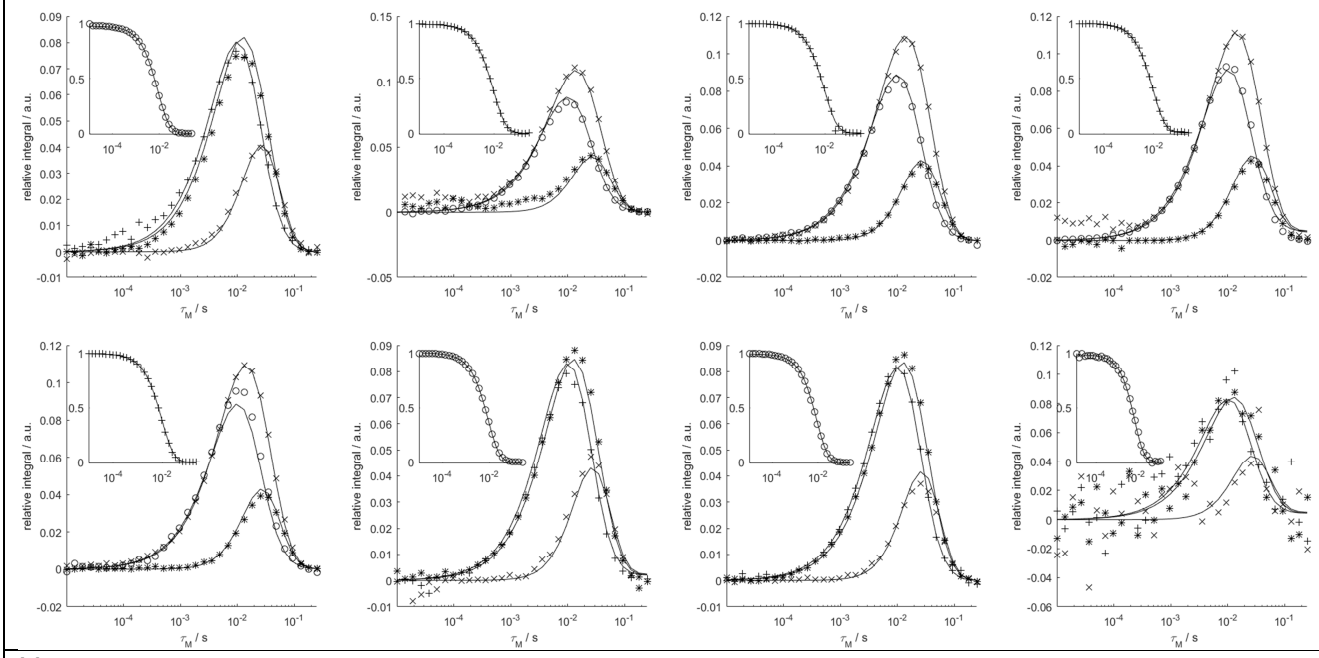

b)

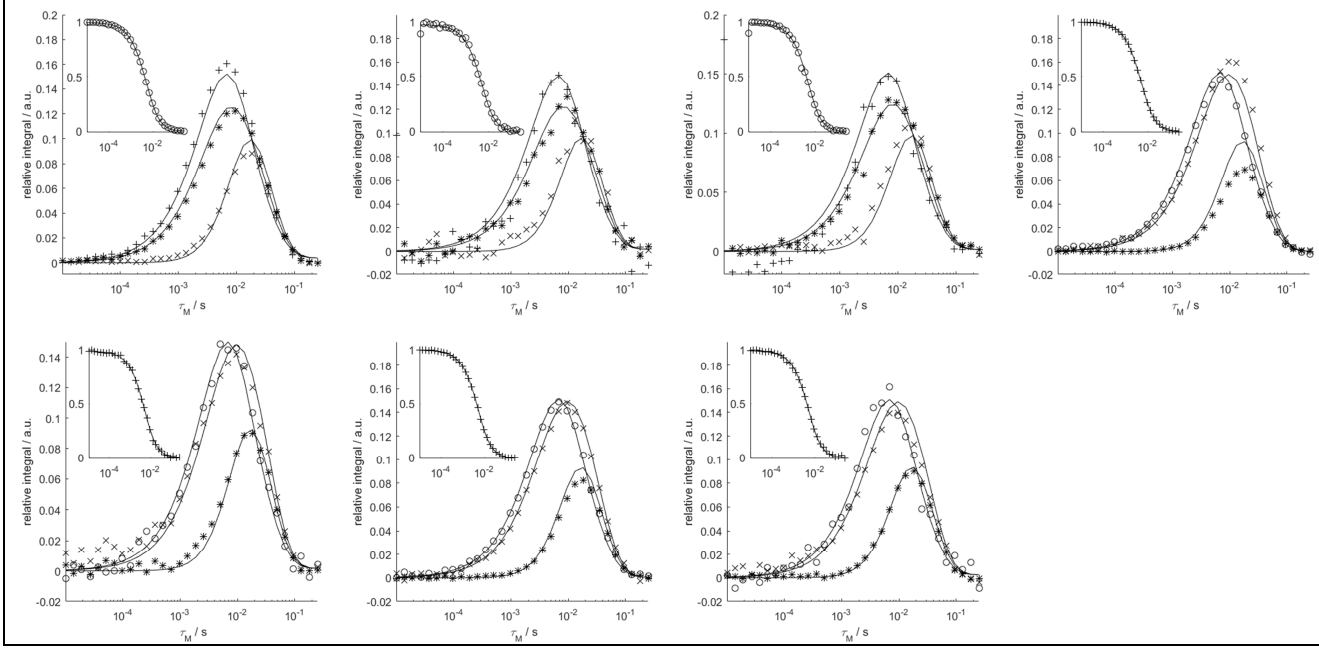

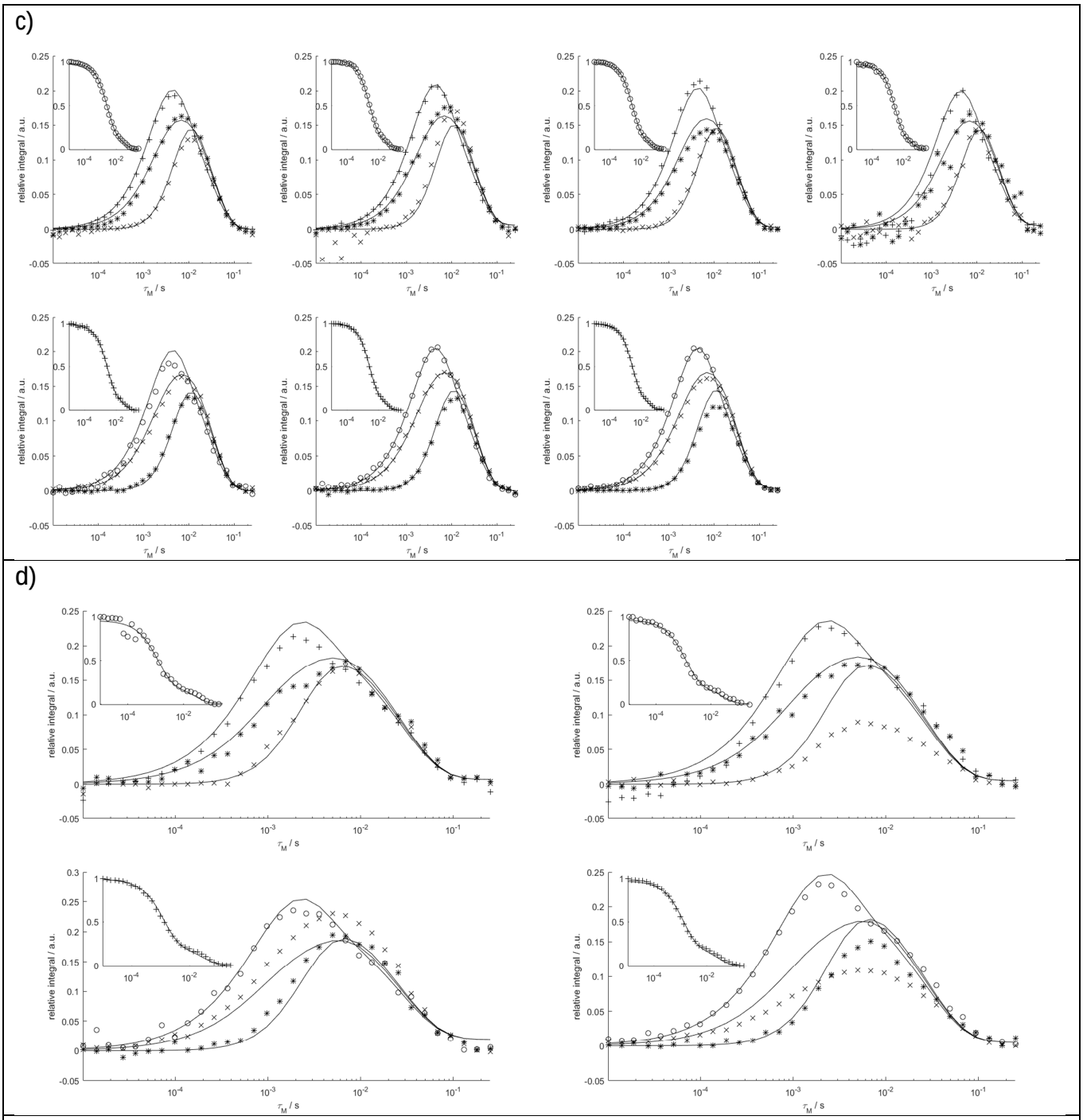

Figure S4. Relative areas of proton NMR signals of $[Eu(Hdo3ap)(D_2O)]^-$ as a function of the mixing time obtained from 1D-EXSY experiments at a) 5 °C b) 15 °C c) 25 °C and d) 35 °C at pD = 3.6. The insets show the evolution of the magnetisation of the signal to which the refocusing selective 180° pulse was applied. Symbols: $TSAP_{ax}$ (+), SAP_{eq} (×), $TSAP_{eq}$ (*), SAP_{ax} (○). The solid lines represent the simultaneous fit of all four data sets using Equation [2].

a)

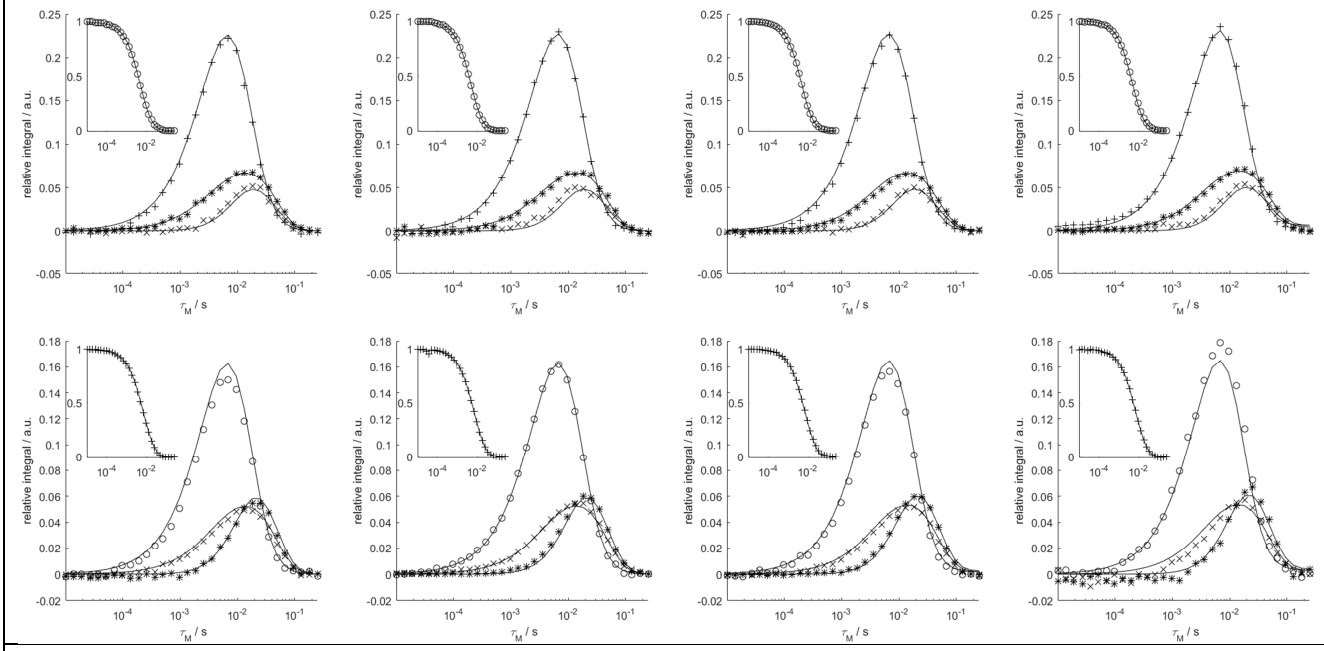

b)

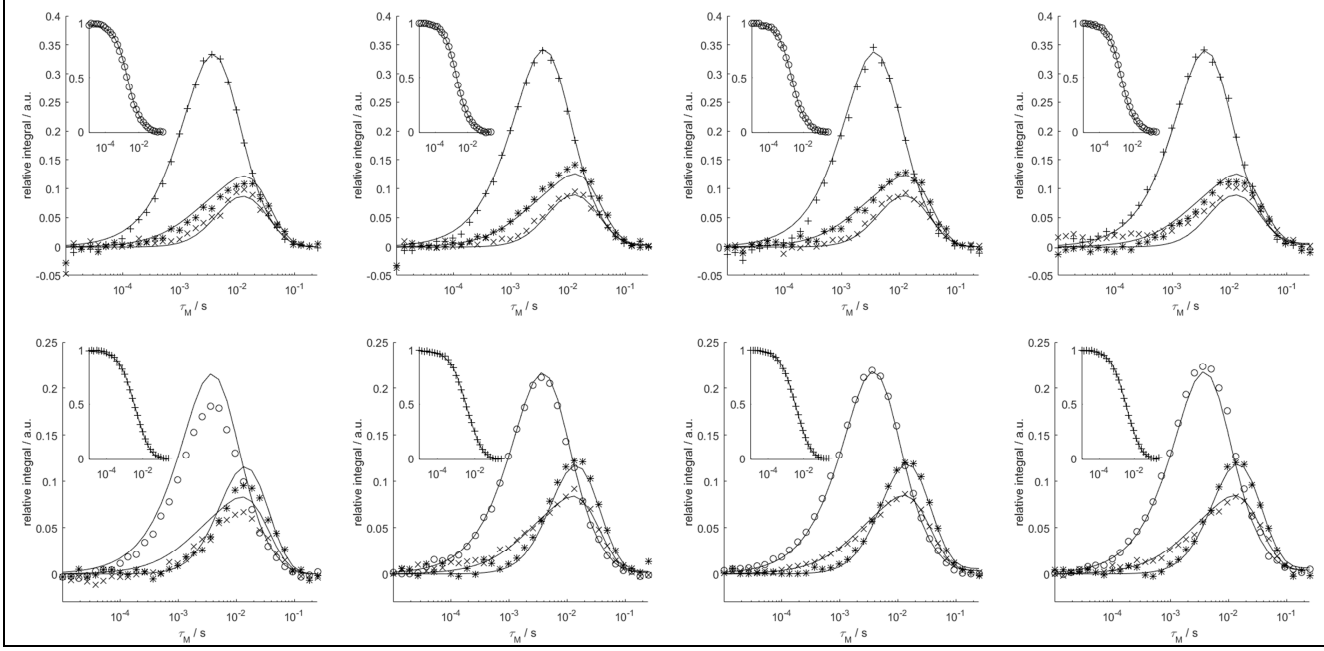

c)

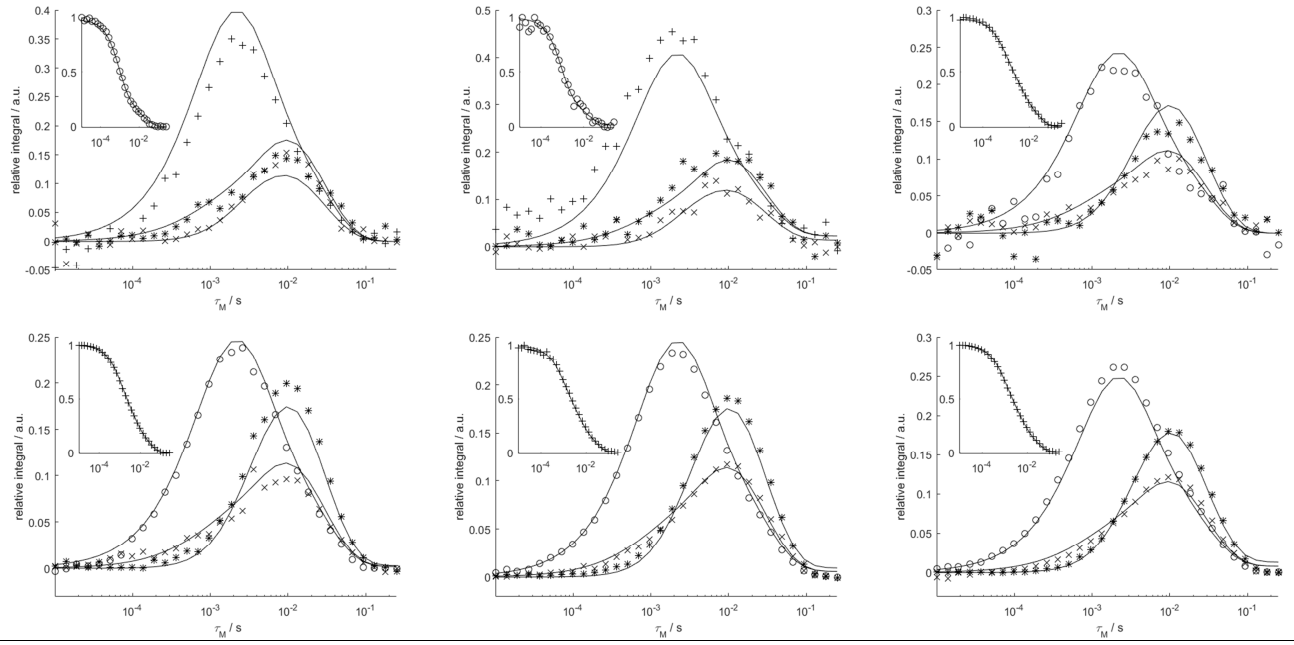

d)

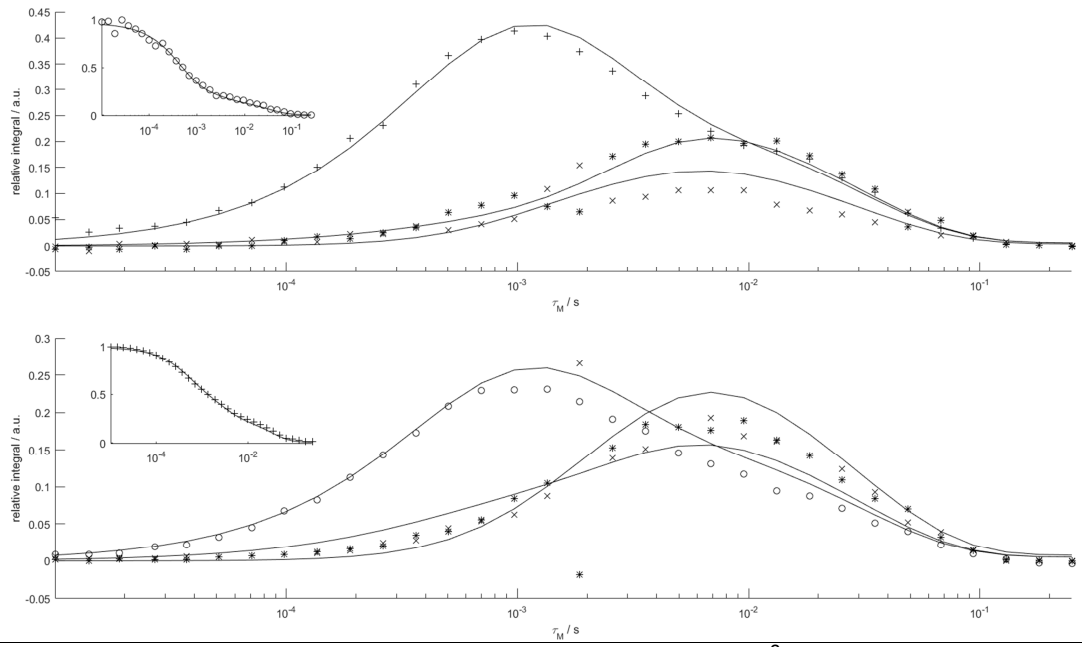

Figure S5. Relative areas of proton NMR signals of $[Eu(do3ap)(D_2O)]^{2-}$ as a function of the mixing time obtained from 1D-EXSY experiments at a) 5 °C b) 15 °C c) 25 °C and d) 35 °C at pD = 8.5. The insets show the evolution of the magnetisation of the signal to which the refocusing selective 180° pulse was applied. Symbols: $TSAP_{ax}$ (+), SAP_{eq} (×), $TSAP_{eq}$ (*), SAP_{ax} (○). The solid lines represent the simultaneous fit of all four data sets using Equation [2].

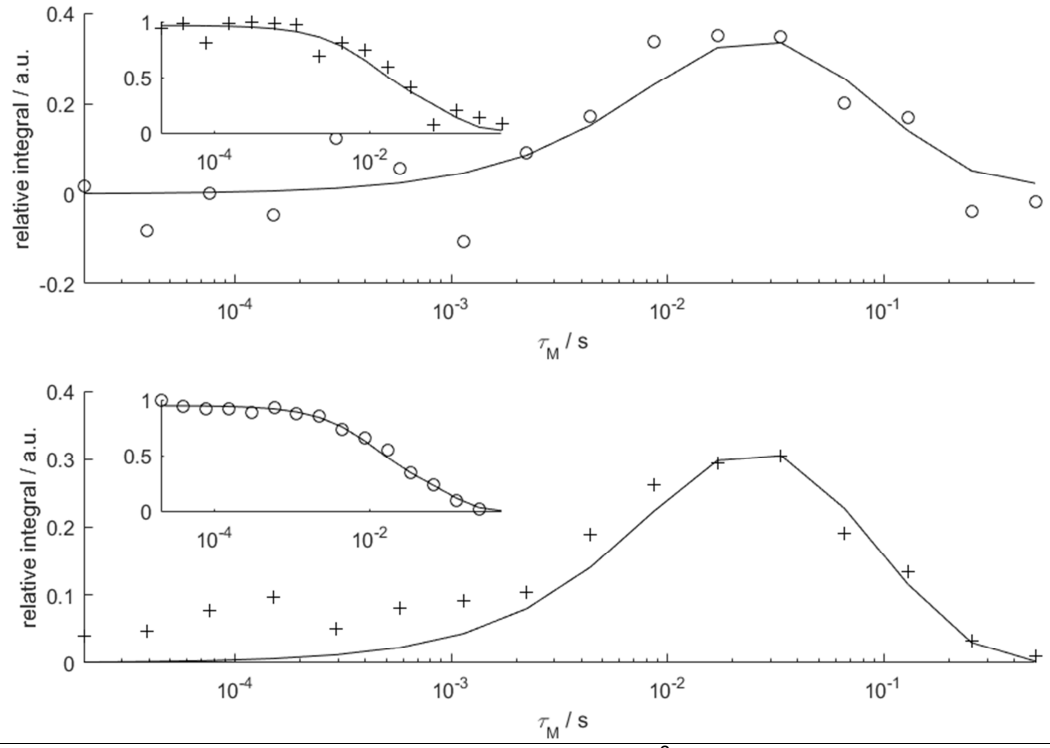

Figure S6. Relative areas of signals of $[Eu(Hdo3ap)(D_2O)]^{2-}$ as a function of the mixing time obtained from ^{31}P 1D-EXSY experiments at 5 °C; pD(25 °C) = 3.6 . The insets show the evolution of the magnetisation of the signal to which the refocusing selective 180° pulse was applied. Symbols: TSAP (+), SAP (○). The solid lines represent the simultaneous fit of both data sets using Equation [2] modified for two-site exchange.

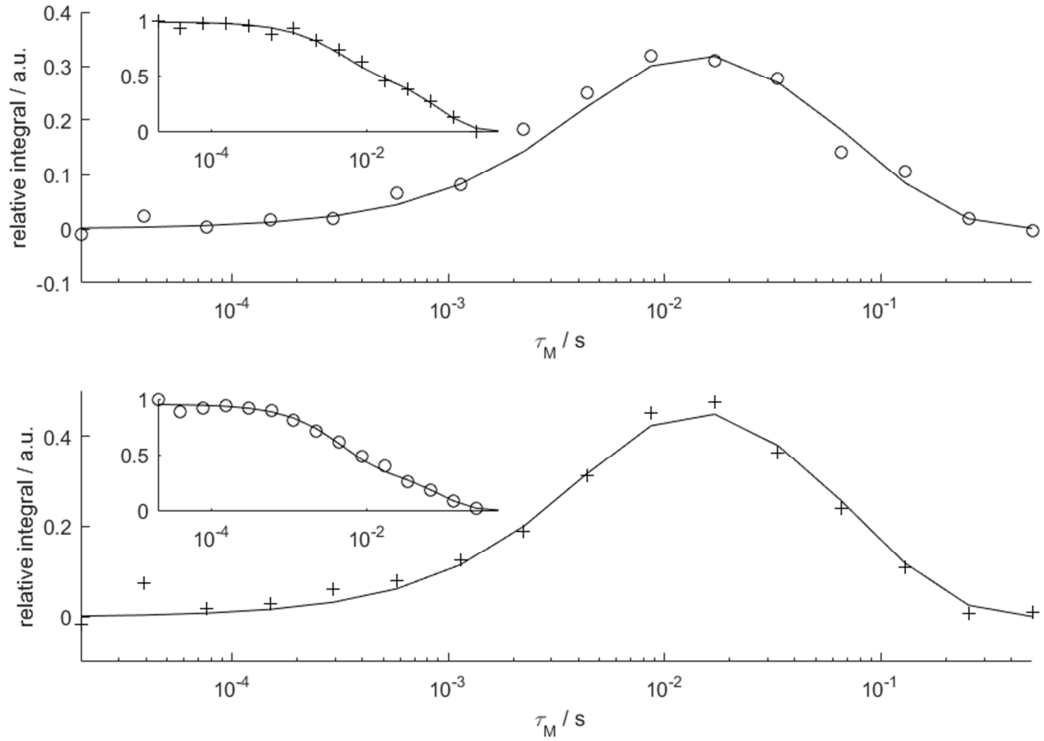

Figure S7. Relative areas of signals of $[Eu(do3ap)(D_2O)]^{2-}$ as a function of the mixing time obtained from ^{31}P 1D-EXSY experiments at 5 °C; pD(25 °C) = 8.5. The insets show the evolution of the magnetisation of the signal to which the refocusing selective 180° pulse was applied. Symbols: TSAP (+), SAP (○). The solid lines represent the simultaneous fit of both data sets using Equation [2] modified for two-site exchange.

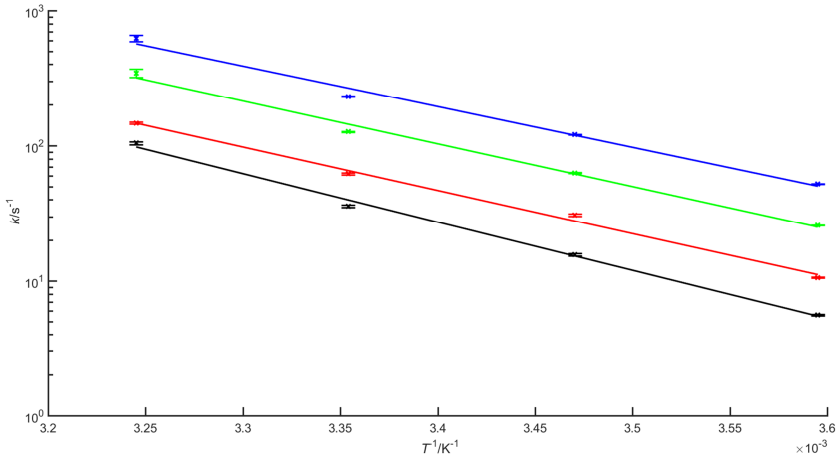

a)

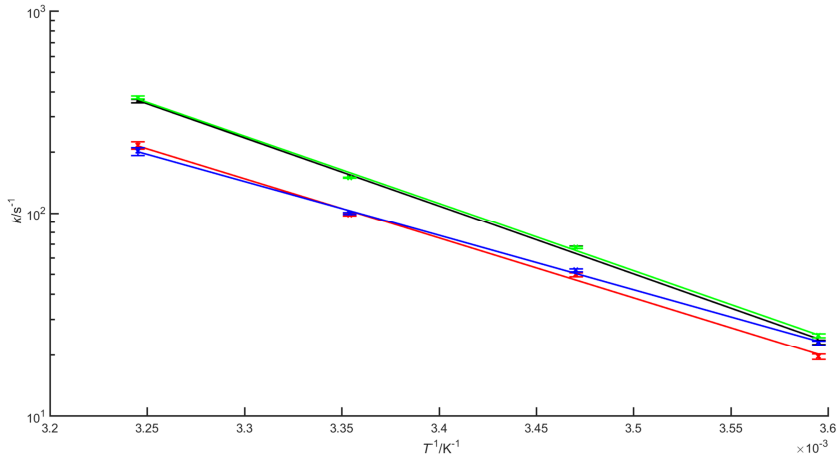

b)

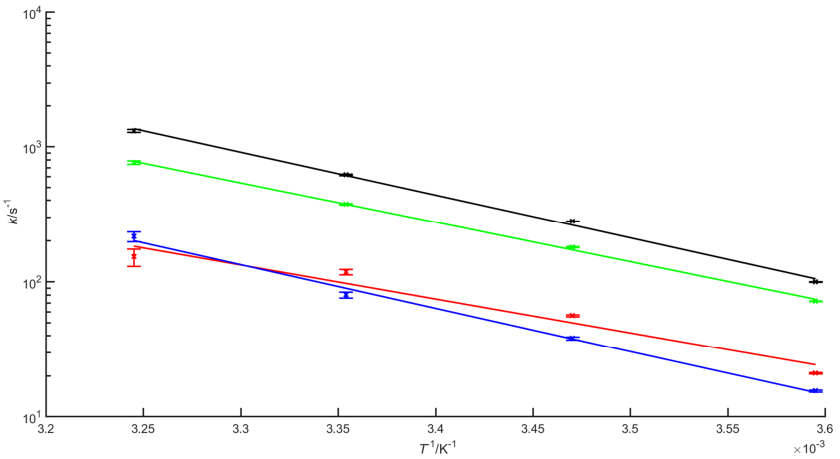

c)

Figure S8: Temperature dependence of exchange rates $k_{PendSAP}$ (black), $k_{CycleSAP}$ (red) , $k_{PendTSAP}$ (green) and $k_{CycleTSAP}$ (blue) of a) $[Eu(dota)(D_2O)]^-$ b) $[Eu(Hdo3ap)(D_2O)]^-$ c) $[Eu(do3ap)(D_2O)]^{2-}$ fitted using Eyring equation (black line) [4].

Table S2: Exchange and relaxation rates of $[Eu(dota)(D_2O)]^{-}$ [a]

Parameter	Temperature / °C			
	5	15	25	35
$k_{PendSAP}$	5.58(6)	15.6(3)	35.8(6)	104(3)
$k_{CycleSAP}$	10.60(7)	30.8(5)	62(1)	147(3)
$k_{PendTSAP}$	25.81(7)	63.0(4)	126.6(9)	345(24)
$k_{CycleTSAP}$	52.30(8)	120.4(5)	231(1)	624(31)
K_{EXSY}	0.207(5)	0.25(1)	0.27(1)	0.26(4)
$R_{1Ax.\ SAP}$	69.1(1)	55.1(6)	43(1)	30(3)
$R_{1Eq.\ SAP}$	22.53(7)	16.2(5)	11(1)	0(5)
$R_{1Ax.\ TSAP}$	47.6(2)	45.9(7)	41(1)	130(25)
$R_{1Eq.\ TSAP}$	18.3(1)	34(4)	54(8)	17(15)

[a] k / s^{-1} are exchange rates, R_1 / s^{-1} are longitudinal relaxation rates and K_{EXSY} is equilibrium constants calculated as $K_{EXSY} = (k_{PendSAP} + k_{CycleSAP})/ (k_{PendTSAP} + k_{CycleTSAP})$.

Table S3: Exchange and relaxation rates of $[Eu(Hdo3ap)(D_2O)]^{-}$ [a]

Parameter	Temperature / °C			
	5	15	25	35
$k_{PendSAP}$	23.2(5)	68(1)	150(1)	357(7)
$k_{CycleSAP}$	19.6(6)	50(1)	98(1)	216(9)
$k_{PendTSAP}$	25.0(5)	67.6(8)	150(1)	374(8)
$k_{CycleTSAP}$	23.0(6)	52.3(9)	100(1)	202(9)
K_{EXSY}	0.89(9)	0.98(7)	0.99(4)	1.0(1)
$R_{1Ax.\ SAP}$	69.4(9)	63(1)	57(1)	68(9)
$R_{1Eq.\ SAP}$	20(3)	8(3)	9(3)	43(29)
$R_{1Ax.\ TSAP}$	54.1(9)	55(1)	52(1)	37(9)
$R_{1Eq.\ TSAP}$	22(3)	32(4)	22(3)	0(28)

[a] k / s^{-1} are exchange rates, R_1 / s^{-1} are longitudinal relaxation rates and K_{EXSY} is equilibrium constants calculated as $K_{EXSY} = (k_{PendSAP} + k_{CycleSAP})/ (k_{PendTSAP} + k_{CycleTSAP})$.

Table S4: Exchange and relaxation rates of $[Eu(do3ap)(D_2O)]^{2-}$ [a]

Parameter	Temperature / °C			
	5	15	25	35
$k_{PendSAP}$	99.7(3)	280(1)	619(8)	1305(30)
$k_{CycleSAP}$	21.0(3)	56(1)	118(5)	152(22)
$k_{PendTSAP}$	71.7(3)	180(1)	374(5)	762(23)
$k_{CycleTSAP}$	15.5(2)	38.2(9)	80(4)	215(18)
K_{EXSY}	1.39(5)	1.54(8)	1.6(2)	1.5(4)
$R_{1Ax.\ SAP}$	73.2(4)	59(1)	42(7)	122(24)
$R_{1Eq.\ SAP}$	16(2)	0(6)	0(29)	0(110)
$R_{1Ax.\ TSAP}$	59.0(3)	63(1)	58(4)	0(19)
$R_{1Eq.\ TSAP}$	23(2)	35(4)	40(18)	32(72)

[a] k / s^{-1} are exchange rates, R_1 / s^{-1} are longitudinal relaxation rates and K_{EXSY} is equilibrium constants calculated as $K_{EXSY} = (k_{PendSAP} + k_{CycleSAP})/ (k_{PendTSAP} + k_{CycleTSAP})$.

Table S5: Exchange and relaxation rates of $[Eu(Hdo3ap)(D_2O)]^{2-}$ and $[Eu(do3ap)(D_2O)]^{2-}$ as determined by ^{31}P 1D-EXSY at 5 °C.[a]

Parameter	$[Eu(Hdo3ap)(D_2O)]^{2-}$	$[Eu(do3ap)(D_2O)]^{2-}$
k_{SAP}	42(3)	120(3)
k_{TSAP}	45(3)	82(3)
K_{EXSY}	0.93(6)	1.46(4)
R_{SAP}	12(3)	7(2)
R_{TSAP}	9(3)	16(2)

[a] k_{SAP} / s^{-1}, k_{TSAP} / s^{-1} are exchange rates of exchange from SAP → TSAP and backward respectively, R_1 / s^{-1} are longitudinal relaxation rates and K_{EXSY} equilibrium constants calculated as $K_{EXSY} = k_{SAP}/k_{TSAP}$. It should be highlighted that arm rotation and cycle inversion cannot be separated by ^{31}P 1D-EXSY as a sum of both processes is observed.

Table S6: Calculated energy profile of cyclen inversion of $[Eu(dota)(H_2O)]^-$. The most favourable pathway is in bold and the rate-determining step is <u>underlined.</u>

Sequence of chelate ring inversions				$\Delta G^{\ddagger}_{calc}$(25 °C) / kJ mol^{-1}								
				SAP	TS 1	int 1	TS 2	int 2	TS 3	int 3	TS 4	TSAP
2	<u>3</u>	4	1	0.00	60.54	19.05	<u>61.99</u>	28.91	57.87	24.77	60.08	–2.84
3	2	4	1	0.00	60.54	21.37	66.90	28.91	57.87	24.77	60.08	–2.84
2	4	3	1	0.00	60.54	19.05	64.48	27.28	63.28	24.77	60.08	–2.84
4	2	3	1	0.00	60.54	21.88	68.08	27.28	63.28	24.77	60.08	–2.84
4	3	2	1	0.00	60.54	21.87	67.01	30.37	72.08	24.77	60.08	–2.84
3	4	2	1	0.00	60.54	21.37	67.42	30.37	72.08	24.77	60.08	–2.84

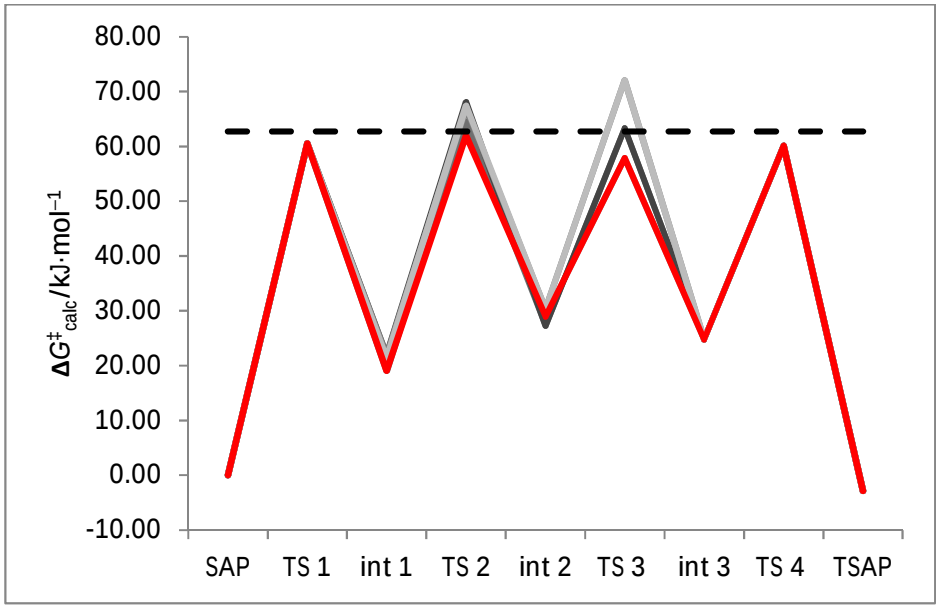

Figure S9: Energy profile calculated for the cyclen inversion of $[Eu(dota)(H_2O)]^-$ at 25 °C. The lowest energy pathway is highlighted in red while the experimental activation free energy is represented by a black dashed line.

Table S7: Calculated energy profile of cyclen inversion of $[Eu(Hdo3ap)(H_2O)]^-$. The most favourable pathway is in bold and the rate-determining step is underlined.

Sequence of chelate ring inversion				$\Delta G^{\ddagger}_{calc}$(25 °C) / kJ mol^{-1}								
				SAP	TS 1	int 1	TS 2	int 2	TS 3	int 3	TS 4	TSAP
1	2	3	4	0	63.6	19.8	64.7	26.9	55.5	19.2	56.8	–2.6
2	1	3	4	0	51.5	19.4	66.2	26.9	55.5	19.2	56.8	–2.6
1	3	2	4	0	63.6	19.8	72.6	32.4	55.0	19.2	56.8	–2.6
3	1	2	4	0	63.7	21.7	69.8	32.4	55.0	19.2	56.8	–2.6
3	2	1	4	0	63.7	21.7	57.5	24.6	65.9	19.2	56.8	–2.6
2	3	1	4	0	51.5	19.4	60.6	24.6	65.9	19.2	56.8	–2.6
1	2	4	3	0	63.6	19.8	64.7	26.9	69.5	23.0	62.3	–2.6
2	1	4	3	0	51.5	19.4	66.2	26.9	69.5	23.0	62.3	–2.6
1	4	2	3	0	63.6	19.8	62.9	25.7	63.0	23.0	62.3	–2.6
4	1	2	3	0	59.6	21.8	71.6	25.7	63.0	23.0	62.3	–2.6
4	2	1	3	0	59.6	21.8	62.8	29.6	66.4	23.0	62.3	–2.6
2	4	1	3	0	51.5	19.4	65.0	29.6	66.4	23.0	62.3	–2.6
1	4	3	2	0	63.6	19.8	62.9	25.7	71.8	27.9	51.7	–2.6
4	1	3	2	0	59.6	21.8	71.6	25.7	71.8	27.9	51.7	–2.6
1	3	4	2	0	63.6	19.8	72.6	32.4	65.7	27.9	51.7	–2.6
3	1	4	2	0	63.7	21.7	69.8	32.4	65.7	27.9	51.7	–2.6
3	4	1	2	0	63.7	21.7	65.5	34.6	67.4	27.9	51.7	–2.6
4	3	1	2	0	59.6	21.8	68.0	34.6	67.4	27.9	51.7	–2.6
4	2	3	1	0	59.6	21.8	62.8	29.6	62.9	20.0	59.4	–2.6
2	4	3	1	0	51.5	19.4	65.0	29.6	62.9	20.0	59.4	–2.6
4	3	2	1	0	59.6	21.8	68.0	34.6	64.0	20.0	59.4	–2.6
3	4	2	1	0	63.7	21.7	65.5	34.6	64.0	20.0	59.4	–2.6
3	2	4	1	0	63.7	21.7	57.5	24.6	56.4	20.0	59.4	–2.6
2	3	4	1	0	51.5	19.4	60.6	24.6	56.4	20.0	59.4	–2.6

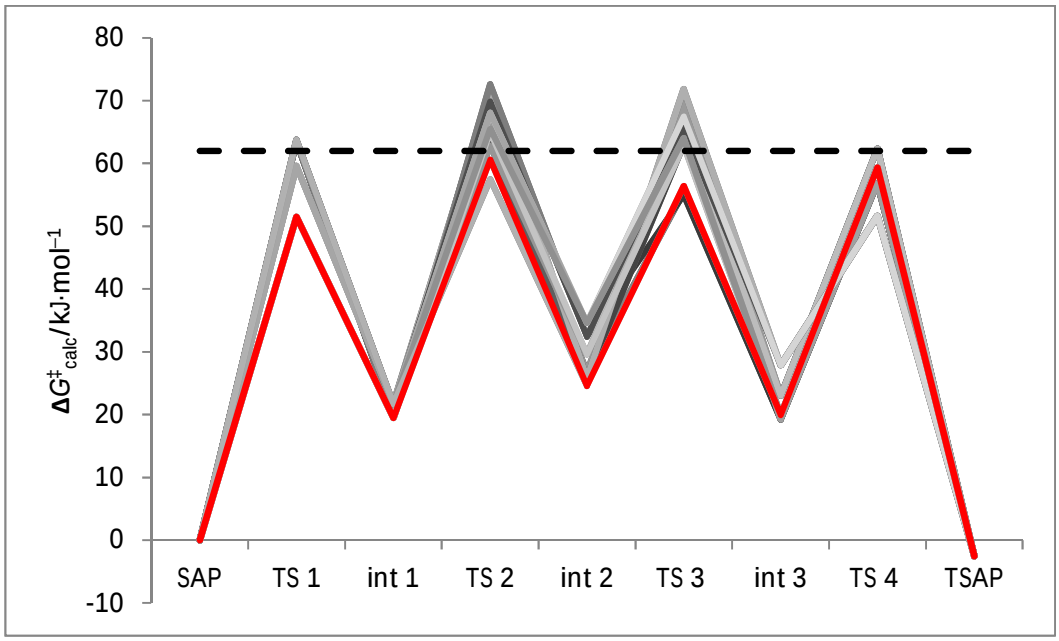

Figure S10: Energy profile calculated for the cyclen inversion of $[Eu(Hdo3ap)(H_2O)]^-$ at 25 °C. The lowest energy pathway is highlighted in red, while the experimental activation free energy is represented by a black dashed line.

Table S8: Calculated energy profile of cyclen inversion of $[Eu(do3ap)(H_2O)]^{2-}$. The most favourable pathway is in bold and the rate-determining step is <u>underlined.</u>

Sequence of chelate ring inversion				$\Delta G^{\ddagger}_{calc}$(25 °C) / kJ mol^{-1}								
				SAP	TS 1	int 1	TS 2	int 2	TS 3	int 3	TS 4	TSAP
4	3	2	1	0.0	68.1	23.9	67.1	30.5	60.2	21.3	49.6	0.9
4	3	1	2	0.0	68.1	23.9	67.1	30.5	62.9	24.1	66.6	0.9
4	2	3	1	0.0	68.1	23.9	71.8	31.8	67.4	21.3	49.6	0.9
4	2	1	3	0.0	68.1	23.9	71.8	31.8	61.1	31.8	67.7	0.9
4	1	2	3	0.0	68.1	23.9	60.5	33.9	81.7	31.8	67.7	0.9
4	1	3	2	0.0	68.1	23.9	60.5	33.9	66.2	24.1	66.6	0.9
3	4	2	1	0.0	64.4	22.4	70.4	30.5	60.2	21.3	49.6	0.9
3	4	1	2	0.0	64.4	22.4	70.4	30.5	62.9	24.1	66.6	0.9
3	2	4	1	0.0	64.4	22.4	67.7	30.4	71.0	21.3	49.6	0.9
3	2	1	4	0.0	64.4	22.4	67.7	30.4	67.8	33.8	65.1	0.9
3	1	2	4	0.0	64.4	22.4	64.1	34.9	70.9	33.8	65.1	0.9
3	1	<u>4</u>	2	0.0	64.4	22.4	64.1	34.9	64.6	24.1	<u>66.6</u>	0.9
2	3	4	1	0.0	71.1	21.1	68.7	30.4	71.0	21.3	49.6	0.9
2	3	1	4	0.0	71.1	21.1	68.7	30.4	67.8	33.8	65.1	0.9
2	4	3	1	0.0	71.1	21.1	77.5	31.8	67.4	21.3	49.6	0.9
2	4	1	3	0.0	71.1	21.1	77.5	31.8	61.1	31.8	67.7	0.9
2	1	4	3	0.0	71.1	21.1	73.5	37.9	63.9	31.8	67.7	0.9
2	1	3	4	0.0	71.1	21.1	73.5	37.9	79.1	33.8	65.1	0.9
1	3	2	4	0.0	57.7	26.3	73.5	34.9	70.9	33.8	65.1	0.9
1	3	4	2	0.0	57.7	26.3	73.5	34.9	64.6	24.1	66.6	0.9
1	2	3	4	0.0	57.7	26.3	81.5	37.9	79.1	33.8	65.1	0.9
1	2	4	3	0.0	57.7	26.3	81.5	37.9	63.9	31.8	67.7	0.9
1	4	2	3	0.0	57.7	26.3	67.2	33.9	81.7	31.8	67.7	0.9
1	4	3	2	0.0	57.7	26.3	67.2	33.9	66.2	24.1	66.6	0.9

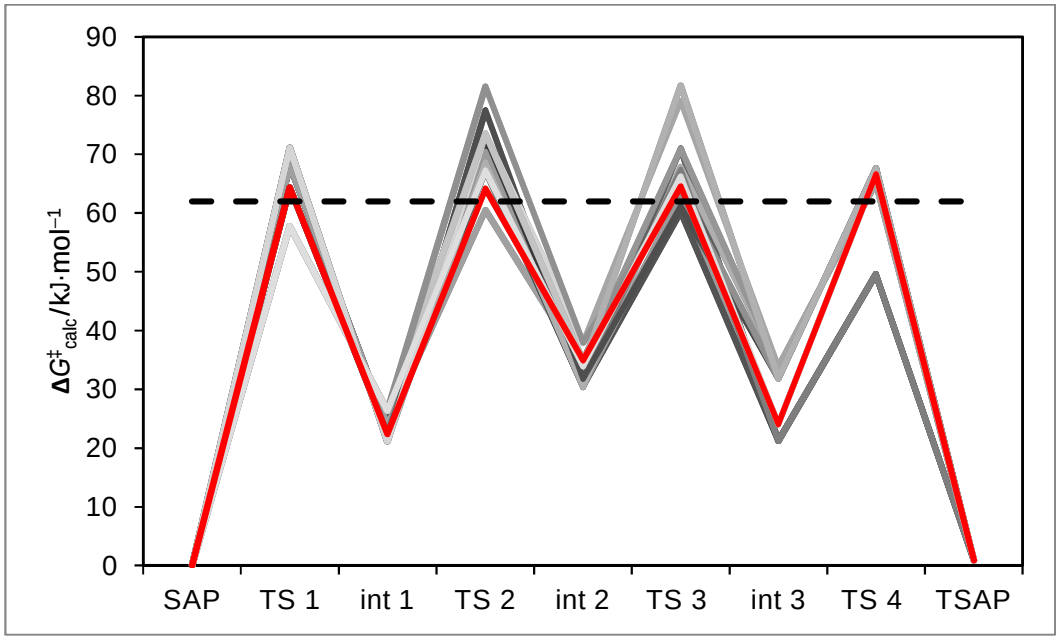

Figure S11: Energy profile calculated for the cyclen inversion of $[Eu(do3ap)(H_2O)]^{2-}$ at 25 °C. The lowest energy pathway is highlighted in red, while the experimental activation free energy is represented by a black dashed line.

Table S9: Contributions to the activation entropy (in J K^{-1} mol^{-1}) for the ring inversion process responsible for the SAP → TSAP interconversion process (at 25 °C).

Anion	$\Delta S^{\ddagger}_{CycleSAP}$		
	Overall	Rotation	Vibration
dota	–3.28	–0.054	–3.23
Hdo3ap	–8.77	0.033	–8.80
do3ap	–14.6	0.12	–14.7

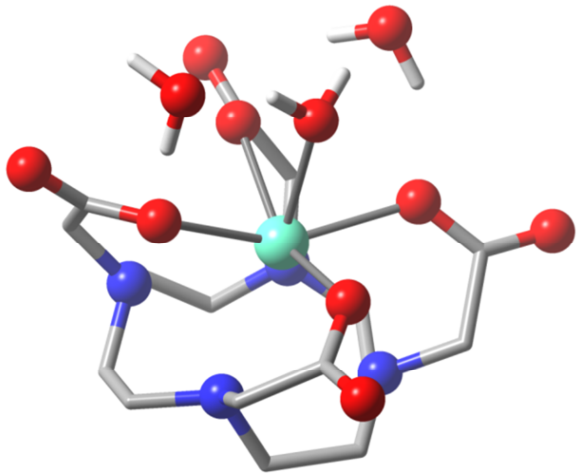

Figure S12. Calculated molecular structure of $[Eu(dota)(H_2O)]^{-}\cdot 2H_2O$ in SAP geometry. Hydrogen atoms bonded to carbon atoms are omitted for the sake of clarity.

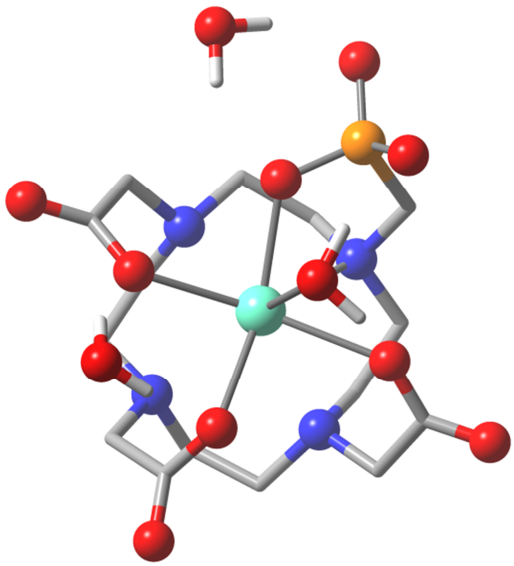

Figure S13. Calculated molecular structure of $[Eu(do3ap)(H_2O)]^{2-}\cdot 2H_2O$ in SAP geometry. Hydrogen atoms bonded to carbon atoms are omitted for the sake of clarity.

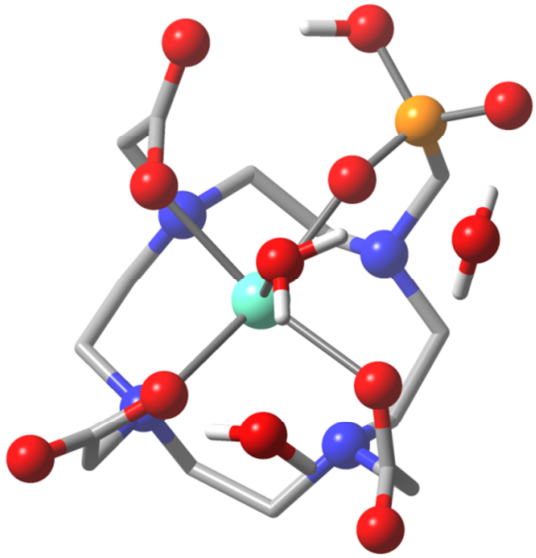

Figure S14. Calculated molecular structure of $[Eu(Hdo3ap)(H_2O)]^{-}\cdot 2H_2O$ in SAP geometry. Hydrogen atoms bonded to carbon atoms are omitted for the sake of clarity.